Exploring hints for dark energy density evolution in light of recent data

Víctor H. Cárdenas
Instituto de Física y Astronomía, Facultad de Ciencias, Universidad de Valparaíso, Gran Bretaña 1111, Valparaíso, Chile and Centro de Astrofísica de Valparaíso, Gran Bretaña 1111, Valparaíso, Chile

Considering a quadratic parametrization of the dark energy density, we explore signatures of evolution using data from gas mass fraction in clusters, type Ia supernova, BAO and CMB. We find – excluding CMB data – a preference for a evolution of $\rho_{de}(z)$ towards smaller values as redshift increases, a result consistent with a recent study using the BAO DR11 data by Delubac et al. (2015).

Keywords: cosmological parameters; cosmology: theory

arXiv:1405.5116v2 [astro-ph.CO] 10 Sep 2015

I. INTRODUCTION

The ΛCDM model is the simplest cosmological model that fits a varied set of observational data; type Ia supernova (SNIa), baryon acoustic oscillations (BAO), Cosmic microwave background radiation (CMBR), growth of structure etc [1]. In this setup the cosmological constant Λ drives the current accelerated expansion of the universe, detected for the first time using type Ia supernovae [2, 3]. Although successful in fitting the data, the model is awkward in many ways: for example, we do not know the mechanism to produce such a constant in the first place. We also do not expect to live in a special epoch where the contribution of this constant is of the same order of magnitude than the non relativistic matter contribution. This problem in particular is known as the "cosmic" coincidence problem.

From a theoretical point of view, it is most natural to think that this contribution comes from an evolving source (with epoch) whose connection with the universe expansion is under study. Dark energy (DE) is the name of this mysterious source [4].

Different DE models have been proposed to provide the mechanism that explains the observational data. There are models where a new field component is assumed to fill the universe, known as quintessence [5–10], and models where the mechanism is triggered by using a modified gravity theory [11–13].

In the absence of consensus regarding a theoretical description for cosmic acceleration, theorists have proposed using the equation of state (EoS) parameter $w(a) = p/\rho$, where a is the scale factor, as a useful phenomenological description [4].

In this context in [14], using the Constitution data set for SNIa [15], and the Chevalier-Polarski-Linder (CPL) parameterization for $w(a)$ [16, 17],

$$w(a) = w_0 + (1 - a)w_1, \tag{1}$$

with w_0 and w_1 being free parameters to be fixed by observations, the authors found a reconstructed deceleration parameter that apparently shows a rapid variation at small redshift around $z \simeq 0.2$. However, once the baryon acoustic oscillations (BAO) and cosmic microwave background (CMB) data are added into the analysis, the best fit result changes completely, showing no sign of variation at the small redshift in agreement with what is expected in the ΛCDM model. In [18] similar results were found, under the assumption of a flat universe using the Union 2 data set [19]. In [20] we revisit this problem using the Union 2 data set extending the analysis to allow for curved spacetime.

In [21], using data from gas mass fraction in galaxy clusters f_{gas}, we encountered the same apparent behavior found previously using SNIa [14, 18, 20].

SNIa are standardizable candles from which we measure the luminosity distance. In the case of the gas mass fraction, we measure the X-ray emission, which enable us to estimate the baryonic (mostly gas) and total mass, assuming the intracluster gas is in hydrostatic equilibrium, from which we measure the angular diameter distance to the cluster [22]. Because the f_{gas} data span a similar redshift range as the SNIa, but depends on a completely different physics, this finding is certainly intriguing.

Although the statistical significance of this effect is small, the consistency between the results using SNIa and f_{gas}, moves us to deepen the study of this effect at low redshift.

We also studied the possible dependence of this result - a low redshift transition of the deceleration parameter - with different parameterizations. In [23] we used five different types of parameterizations and the result was always consistent with that found using CPL. However, the analysis based on using $w(z)$ increases the errors in the parameters we want to constrain. The problem with using $w(z)$ as the focus of study was demonstrated in [24] (see also [25]). The essential problem is the observational quantity, as the luminosity distance or the angular diameter distance, depends on $w(z)$ through a double integral smearing out the information about $w(z)$ itself and its time variation.

As the ΛCDM model is by definition a model with a constant DE density, in this work we focus on signals of a possible departure from this trend. In this context, as was explained in the previous paragraph, is not efficient to use $w(z)$ or a particular parametrization of it; instead, we work directly with the dark energy density, whatever that may be. This strategy was started in [26], and [27], where the authors demonstrated the advantage of using the energy density instead of the EoS parameter as the

main probe to constraint.

In this paper we investigate the possibility of evolution of the dark energy density in light of recent data. We use gas mass fraction in clusters [22] - 42 measurements of f_{gas} in clusters extracted from [28] - and also type Ia supernovae (SNIa) from the Lick Observatory Supernova Search (LOSS) compilation sample [29]. We also consider the constraints obtained from BAO and CMB. The BAO measurements considered in our analysis are obtained from the WiggleZ experiment [39], the SDSS DR7 BAO distance measurements [40], and 6dFGS BAO data [41]. We also include background CMB information by using the Planck data [30] to probe the expansion history up to the last scattering surface. We have also perform the analysis using the WMAP 9-yr covariance matrix from [42], with no significant changes.

The paper is organized as follows: in the next section we describe what we have learned from the $w(z)$ parametrization. Then, we describe how to implement the interpolation method to constrain the DE density model using the observational data available. After that, we present the results of our study, first using SNIa and f_{gas} data and then within a joint analysis. We end with a discussion of the results.

II. INSIGHTS FROM THE RECONSTRUCTED DECELERATION PARAMETER

Observational cosmology is essentially based on quantities derived from the Hubble function. For example, using both type Ia supernova or galaxy cluster data, the key functions are written in terms of the comoving distance from the observer to the redshift z given by

$$r(z) = \frac{c}{H_0}\frac{1}{\sqrt{-\Omega_k}}\sin\sqrt{-\Omega_k}\int_0^z \frac{dz'}{E(z')}, \qquad (2)$$

where $E(z) = H(z)/H_0$ contains the cosmology. For example, for the case of the ΛCDM model the function is,

$$E^2(z) = \Omega_m(1+z)^3 + \Omega_r(1+z)^4 + \Omega_k(1+z)^2 + \Omega_\Lambda. \quad (3)$$

Here Ω_m comprise both the baryonic and non baryonic DM. We know the radiation component is negligible at low redshift; in fact, we know $h^2\Omega_r = 2.47\times10^{-5}$ from [30]. However, if we want to constrain our model using data from BAO and CMB, we have to use it, because these probes refers to both the last scattering redshift and the drag epoch.

In practice, by using the CPL parameterization (1) for the DE component, and after testing it against the observational data, we get the best fit values of the parameters, which give us the best Hubble function $E(z) \equiv H(z)/H_0$ that agrees with the data. From it, following previous works [14, 18, 20], we reconstruct the deceleration parameter function

$$q(z) = (1+z)\frac{1}{E(z)}\frac{dE(z)}{dz} - 1. \qquad (4)$$

TABLE I: The best fit values for the free parameters using SNIa + f_{gas}. See also Fig. 1.

h	Ω_m	w_0
0.695±0.004	0.30±0.04	-0.73±0.16
w_1	Ω_b	b
-2.7±1.5	0.0457±0.0008	0.84±0.09

In order to motivate the next section, we will repeat the calculation with recent data. We use gas mass fraction in clusters extracted from [28], and also type Ia supernovae (SNIa) from the LOSS compilation sample [29]. From now on we assume a spatially flat universe ($\Omega_k = 0$).

The SNIa data give the luminosity distance $d_L(z) = (1+z)r(z)$. We fit the SNIa with the cosmological model by minimizing the χ^2 value defined by

$$\chi^2_{SNIa} = \sum_{i=1}^{586}\frac{[\mu(z_i) - \mu_{obs}(z_i)]^2}{\sigma^2_{\mu i}}, \qquad (5)$$

where $\mu(z) \equiv 5\log_{10}[d_L(z)/\mathtt{Mpc}] + 25$ is the theoretical value of the distance modulus, μ_{obs} is the corresponding observed one, and $\sigma_{\mu i}$ is the error associated to it. As explained in [29], the error comprises three components: the uncertainty from light-curve fits, a component due to the peculiar velocity of each SNIa, and an intrinsic scatter term which depends on the sample (see Table 1 in [29]).

The gas mass fraction data we use span a redshift range $0.05 < z < 1.1$. The f_{gas} data are quoted for a flat ΛCDM reference cosmology with $h = H_0/100$ km s^{-1}Mpc^{-1} = 0.7 and $\Omega_M = 0.3$. To obtain the restrictions we use the model function from [31]:

$$f_{gas}^{\Lambda CDM}(z) = \frac{b\Omega_b}{(1+0.19\sqrt{h})\Omega_M}\left[\frac{d_A^{\Lambda CDM}(z)}{d_A(z)}\right]^{3/2}, \quad (6)$$

where b is a bias factor motivated by gas-dynamical simulations which suggest the the baryon fraction in clusters is slightly lower than for the universe as a whole. From [32] $b = 0.824 \pm 0.0033$ is obtained. Following [31] we adopt a gaussian prior on b, taking into account systematic uncertainties, so we use $b = 0.824 \pm 0.089$. In the analysis we also use standard Gaussian priors on $\Omega_b h^2 = 0.02205\pm0.00028$ and $h = 0.72\pm0.08$ from Planck and WMAP polarization [30].

The use of SNIa and f_{gas} data separately, as demonstrated in [21], generates a behavior that is consistent between them. For that reason, in what follows we show first the result considering both probes together. Given the two data sets are consistent each other, we use the standard χ^2 analysis.

In the analysis (see the details in Appendix A) we consider $h, \Omega_m, w_0, w_1, \Omega_b$ and b as free parameters. As we mentioned, we have added Gaussian priors for h, Ω_b and b. After the analysis the best fit values are those shown in Table I.

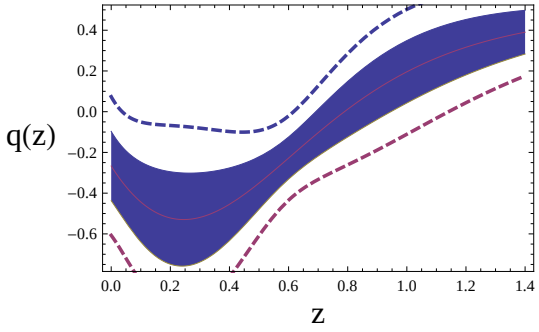

FIG. 1: Using the LOSS compiled sample by [29] and the f_{gas} data from [31] we plot the reconstructed deceleration parameter (4) using the best fit values for the CPL parametrization. We consider the error propagation at one and two sigmas in the best fit parameters. We observe a hint for a low redshift transition, reaching the maximum acceleration around $z \simeq 0.2$, and later a slowing down of the acceleration. The shaded region is 1σ and the region between the dashed lines is 2σ.

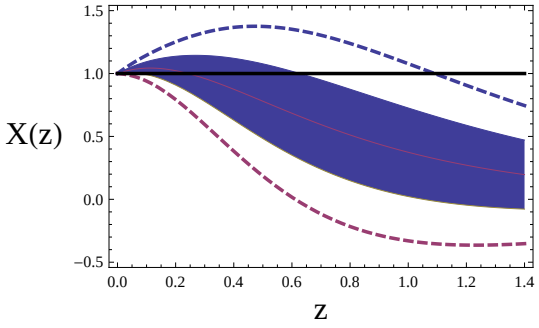

FIG. 2: Using the SNIa and the gas mass fraction data used in the previous analysis we plot the DE density (7) reconstructed using the best fit values for the CPL parametrization. We consider the error propagation at one and two sigmas in the best fit parameters. We observe a preference for a decaying DE density with increasing redshift.

Using the best fit values for the CPL parameters (w_0, w_1), the deceleration parameter (4), with error propagation, is shown in Fig.1. From figure 1, we notice that the combined action of SNIa and f_{gas} data suggest a universe in transit, from a decelerated expansion regime to an accelerated one, with the transition redshift $z \simeq 0.8$, in agreement with ΛCDM, and also a slowing down of the acceleration at recent times, a result that seems to be supported at a 2σ level.

It is important to stress here that the support for this low redshift behavior disappears once we consider BAO and CMB data. This result gives us a hint that seems to indicate a tension between low and high redshift probes.

The key result here, which as far as we know no one has mentioned to date, is that in all the previous cases studied [18, 20, 21] showing a reconstructed deceleration parameter with a rapid variation at the small redshift, i.e. using SNIa and f_{gas} data only, the reconstructed DE density appears to be a decreasing function with increasing redshift at 2σ.

In fact, in the special case of the CPL parametrization for $w(z)$ Eq.(1), we find that

$$X(z) \equiv \frac{\rho_{de}(z)}{\rho_{de}(0)} = e^{-\frac{3w_1 z}{1+z}}(1+z)^{3(1+w_0+w_1)}, \qquad (7)$$

which can be interpreted as a very special parametrization for the DE density. The best fit values of the parameters enable us to get the Hubble function $E(z)$ and the DE density from (7). We have checked that the same trend (at 2σ level) is obtained by using both the Constitution data set and the Union 2 set together with the gas mass fraction data [31].

Here, using recent SNIa data and f_{gas} data, we have reconstructed the DE density from (7) and displayed it in Fig.2. The data through the CPL parametrization seems to suggest an evolving DE density at a 2σ level.

In what follows we test whether the behavior that seems to suggest the low-redshift data – a decreasing DE density with increasing redshift using a parametrization for $w(z)$ – persist, once we consider a parametrization for the DE density.

III. THE METHOD

In order to explore the eventual redshift evolution of the DE density, we use as a probe the definition $X(z) = \rho_{de}(z)/\rho_{de}(0)$, and write the Hubble function as

$$E^2(z) = \Omega_m(1+z)^3 + \Omega_r(1+z)^4 + \Omega_X X(z), \qquad (8)$$

where $\Omega_r = 2.47 \times 10^{-5} h^{-2}$ and $\Omega_m + \Omega_r + \Omega_X = 1$. In the case of using the CPL parametrization Eq.(1), we have already found the expression (7).

In this work we use the method suggested by [26], [27], and extended by [33], parameterizing the DE density through a quadratic interpolation with two free parameters. In this work we restrict ourselves to this number of free parameters, just to compare with previous ones [38] and maintain a meaningful statistical analysis. In assuming a quadratic function for $X(z)$, it is convenient to define the free parameters in reference to the maximum redshift value in the data. In this case we use

$$X(z) = 1 + \frac{z(4f_1 - f_2 - 3)}{z_m} - \frac{2z^2(2f_1 - f_2 - 1)}{z_m^2}, \qquad (9)$$

where z_m is the maximum redshift value in the data, and the free parameters are: $f_1 = X(z_m/2)$ and $f_2 = X(z_m)$. If there is no evolution, i.e. a cosmological constant is preferred, both parameters should have to be equal to unity.

TABLE II: For each one of the data sets we display the distance from the best fit point (see the definition in Eq. (10)) in the two-dimensional space (f_1, f_2), from the ΛCDM model. See also Fig. 3.

Set	d_σ	Ω_m	f_1	f_2
SNIa	2.46	0.299	0.627	-0.635
f_{gas}	1.896	0.293	0.196	-2.622
CMB	1.107	0.256	0.503	0.509
BAO	0.976	0.262	0.637	0.049

IV. RESULTS

To start the analysis, we test the parameterized DE density (9) for each of the observational probes separately. The idea here is to clarify what kind of trend suggests the use of each of the different data sets considered in this work, and also evaluate the consistency among them. In what follows we have used $z_m = 1.34$, which is the highest redshift in our data. We have tried different values for z_m and find no variation in the qualitative behavior.

To study the consistency among the different data sets with the ΛCDM model, we follow the method proposed in [34], where a distance d_σ (in units of σ) from the best fit point to the ΛCDM model, is defined through the relation

$$1 - \Gamma(1, \Delta\chi^2/2)/\Gamma(1) = \texttt{Erf}(d_\sigma/\sqrt{2}), \qquad (10)$$

where the left hand side is the cumulative distribution function (for two parameters), and $\Delta\chi^2 = \chi^2_{(f_1,f_2)} - \chi^2_{min}$ is the χ^2 difference between the best fit and the ΛCDM point ($f_1 = f_2 = 1$).

Using the LOSS compiled sample [29] of SNIa, assuming a flat universe ($\Omega_k = 0$) with the free parameters being, Ω_m, h, f_1, f_2, we obtain a distance $d_\sigma = 2.46\sigma$ away from the reference point ($f_1 = f_2 = 1$): the ΛCDM model. Using the gas mass fraction f_{gas} data from [28], with the free parameters being Ω_m, h, f_1, f_2, Ω_b and b, and using the same priors on b and Ω_b mentioned in section II, we obtain a distance $d_\sigma = 1.896\sigma$ away from the reference point ($f_1 = f_2 = 1$). Using the BAO data, with Ω_m, h, f_1, f_2, and Ω_b as free parameters, we obtain a distance $d_\sigma = 0.976\sigma$ away from the reference point ($f_1 = f_2 = 1$). Using the CMB data, with the same free parameters as in the BAO set, we get $d_\sigma = 1.107\sigma$ away from the ΛCDM model. A summary of our results are shown in table II.

Notice the best fit values of Ω_m for each data set. The DE evolution model we are testing prefer rather lower values for Ω_m ($\simeq 0.26$) once we test it against BAO and CMB data. This fact makes these data sets consistent each other. Meanwhile, using SNIa and f_{gas}, the DE evolution model takes values $\Omega_m \simeq 0.3$. A reconstruction of the DE density for each one of the data sets is plotted in Fig. 3. On the one hand, from the figure it is clear the similarity in the result between SNIa and f_{gas}.

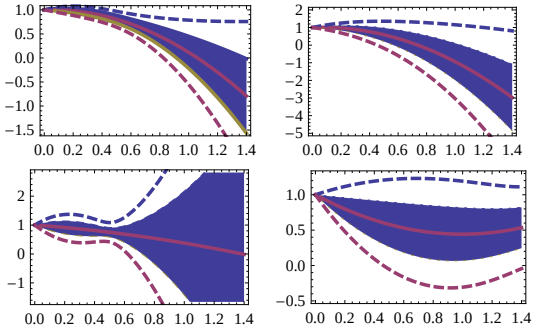

FIG. 3: The horizontal axes indicate the redshift z and the vertical axes indicate $X(z)$. The upper left graph is reconstructed using SNIa data, the upper right graph was obtained using f_{gas} data, the lower left graph is based on BAO data, and the lower right is obtained using CMB data. All the graphs show $X(z)$ as a function of redshift, with error propagation at one (shaded area) and two (dahed lines) sigmas. Notice the trend of a decaying DE density with redshift in the case of SNIa and f_{gas}.

Under general considerations (neglecting an initial mild increase in $X(z)$) we obtain a reconstructed DE density evolving, apparently decreasing as the redshift increases. In this sense, these two probes are consistent each other. On the other hand, both the results using with BAO and CMB are essentially consistent with a cosmological constant even at one sigma, thus being inconsistent with the previous two probes.

This result is actually what we have taken into account in the analysis performed in [21], where we separate the analysis using first SNIa + f_{gas} and then all the probes together. In what follows, we adopt the same procedure starting with a joint analysis between SNIa + f_{gas}, and after that a joint analysis with all the data set together.

First, using the LOSS compiled sample [29] and the gas mass fraction f_{gas} data from [28], we obtain the best fit values of the model (9), assuming a flat universe ($\Omega_k = 0$) with the free parameters being, Ω_m, h, f_1, f_2, Ω_b and b.

Using these data together, using the same priors on b and Ω_b mentioned in section II, we find the best fit values shown in Table III. We plot the DE density as a function of redshift in Fig.(4), with error propagation at one and two sigmas. Here we have taken into account the correlation error between the parameters f_1 and f_2. Note that at one and two sigmas, the reconstructed DE density appears to decrease with increasing redshift.

Obtaining a decreasing DE density as the redshift increases, as the one obtained here, would eventually lead us to get negative values for $X(z)$, as can be observed in Fig. 4 for $z > 0.8$. Although this idea may seem contrary to common sense, a negative DE density has been considered in the past. For example, in [35] the author considered a model inspired from unimodular gravity, predicting fluctuations in the cosmological constant. These fluctuations of the cosmological "constant" are al-

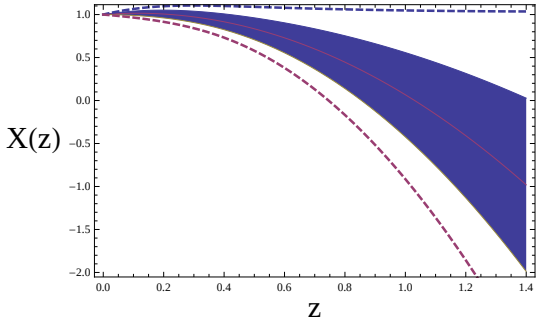

FIG. 4: Adopting the best fit parameters obtained from using the LOSS compilation by [29] of SNIa together with the gas mass fraction data from [31] (see Table III), we plot the DE density as a function of redshift, with error propagation at one (shaded area) and two (dahed lines) sigmas, including error correlation between the parameters f_1 and f_2. Notice the intriguing result of a decaying DE density with redshift.

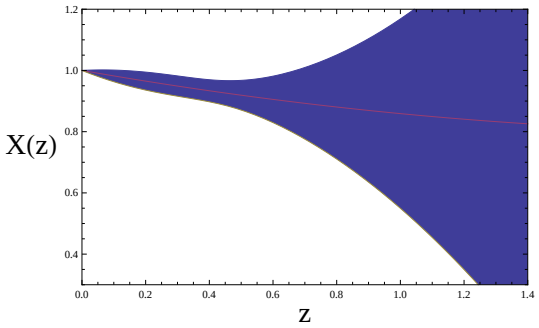

FIG. 5: Adopting the best fit parameters from the analysis using SNIa + f_{gas} + BAO + CMB, we plot the DE density as a function of redshift, with error propagation to one sigma including error correlation between the parameters f_1 and f_2. The result shows that the addition of these probes makes the reconstructed DE density $X(z)$ consistent with no evolution.

TABLE III: The best fit values for the free parameters using (1) SNIa + f_{gas}, and (2) SNIa + f_{gas}+BAO+CMB. See also Figs. 4, and 5.

Set	h	Ω_m	f_1
(1)	0.698±0.004	0. 29±0.03	0.65±0.22
(2)	0.704±0.004	0.273±0.009	0.87±0.10
Set	f_2	Ω_b	b
(1)	-0.75±0.93	0.0453 ±0.0007	0.83±0.06
(2)	0.89±0.64	0.0457±0.0008	0.79±0.03

ways of the order of the ambient density, and it is not strange that Λ may eventually take negative values. Also in this context and using the back-reaction approach the author of [36] obtains a cosmological constant which oscillates about 1/2 the total Ω on Hubble time scales. It is also interesting to mention the work done in [37]. There the authors performed a study of an interacting DM/DE model using a moderately general interaction term. One of their conclusions was that, based on their examples, a solution to the coincidence problem would require that the DE density should take negative values in the past.

Once we consider the data from BAO and CMB together with the already described SNIa and f_{gas}, we minimize the joint chi square, $\chi^2 = \chi^2_{SNIa} + \chi^2_{BAO} + \chi^2_{CMB} + \chi^2_{fgas}$, where each element is defined in appendix A. In the conventional joint χ^2 analysis, we weight each probe equally. This may be problematic if two data sets are mutually inconsistent [43]. A well-motivated approach to assigning weights is the "hyper-parameter" method [43, 44]. In this approach, finding the best-fitting parameters requires us to minimize an effective χ^2 given by

$$\chi^2_{hy} = \sum_i N_i \ln \chi^2_i, \tag{11}$$

where i sums over all the data sets (i = SNIa, BAO, CMB, fgas), and N_i is the number of data points in each data set. Once the χ^2 values have been obtained, we find the posterior distribution for the parameters using the conventional χ^2 or the hyper-parameter version χ^2_{hy} [44]. The results are shown in Table III.

A quadratic parametrization of this type was used by [38], where the authors used a sample with 192 SNIa in combination with CMB and LSS data. Unfortunately, the authors did not show the result using only SNIa data. When comparing their results with our analysis, considering SNIa, f_{gas} and both BAO and CMB data, our results show smaller uncertainties and are more consistent with no change compared with them. In fact, their results indicate a growing DE density with redshift at one sigma. We plot the DE density as a function of redshift in Fig.(5), with error propagation at one sigma. It is very clear that the addition of BAO and CMB data makes the evidence of evolution disappears. This is exactly what we discussed at the end of Section II, in the context of a CPL parameterization for $w(z)$. At this point it seems there is an intriguing connection between the previously found low redshift transition of the deceleration parameter $q(z)$, and a DE density $X(z)$ that decreases as the redshift increases.

It is also interesting to mention that such a behavior – a low redshift transition of the deceleration parameter $q(z)$ (4) – was previously found first (as far as we know) by [45] in the context of Lemaitre-Tolman-Bondi inhomogeneous models. In that work, and in recent ones [46, 47], the authors derived an effective deceleration parameter for void models, indicating that such a behavior of $q(z)$ may be considered a signature for the existence of voids.

Furthermore, a decreasing DE density with increasing redshift is also found in the recent BAO data release by [48], where a tension between BAO data and CMB is found. This tension reveals that in order to accommodate these new data it is not sufficient to go into models with non-zero curvature or a constant $w \neq -1$ DE, essentially because the data requires a decreasing $D_A(z = 2.34)$ while increasing $D_H(z = 2.34)$. The intriguing result,

assuming a flat universe with dark matter and DE is that (quoted from [48])

$$\frac{\rho_{de}(z=2.34)}{\rho_{de}(z=0)} = -1.2 \pm 0.8, \tag{12}$$

which shows this data seems to favor an evolving DE density as we have found in this work using SNIa and f_{gas}.

An evolving DE density, as seems to be suggested by our study, not only means that the DE contribution itself varies with time. This may also be produced by other means. For example, it can be produced by a locally inhomogeneous distribution of matter, like the previously mentioned example using LTB models. Also, as we have mentioned on our discussion on negative DE density, this can also be obtained by assuming an explicit interaction between DM and DE (see for example [37]).

After having uploaded a draft version of this paper to the web [54], several works have appeared whose results point in the same direction. In [55] the authors use the BAO data from the BOSS DR11 [48], along $H(z)$ measurements at low redshift, finding a considerable tension with the standard ΛCDM model, implying a evolution for DE. Also in [56], the authors use the same data from BOSS to show that such a departure from the ΛCDM model can be accommodated assuming an interaction between dark matter and DE, excluding the null interaction at 2σ.

V. DISCUSSION

In this paper we have presented a study of possible signs of evolution of the DE density in light of recent data. We use gas mass fraction in clusters - 42 measurements of f_{gas} in clusters extracted from [28] - and also type Ia supernovae data compiled in [29] from the LOSS team. We also consider the constraints obtained by adding measurements from baryon acoustic oscillations (BAO) and cosmic microwave background radiation (CMB). We have found – using SNIa and f_{gas} data – evidence that relates the previously found low redshift transition of the deceleration parameter to a decreasing DE density evolution with increasing redshift. This result seems to confirm the tension between the data at low redshift and those from CMB. This result is also consistent with a recent anisotropic BAO measurement of BOSS DR11 [48], which shows that the data appear to prefer a decreasing DE density with increasing redshift.

Although the statistical significance of the result is low – this manifests up to 2σ – it is interesting to focus on what the low redshift data are telling us. Because we expect the DE component to be dominant at recent (low redshift) epoch, and the fact that now data from SNIa, gas mass fraction and the recent BAO DR11 results all seem to agree on this peculiar behavior at low redshift, we may conclude that something in our near neighborhood is producing this result. This conclusion is also reinforced with the intriguing similarity between our finding and the result using LTB inhomogeneous model, where the effective deceleration parameter shows the same transition at low redshift, assuming we live inside a void. In summary, the analysis in this work suggests either (i) we live inside a void, or (ii) there is an evolving DE model that produces rapid changes at low redshift. So, it is clear that a careful study of low redshift behavior is needed to enlighten our understanding of DE.

Acknowledgments

The author wishes to thank Yoelsy Leyva, Juan Magaña and Sergio del Campo for useful discussions. This work was funded by the Comisión Nacional de Ciencias y Tecnología through FONDECYT Grant 1110230 and DIUV 50/2013.

[1] L.Perivolaropoulos, Journal of Physics: Conference Series, 222, 1, 012024,2010
[2] A.G. Riess et al., AJ, 116, 1009, 1998
[3] S. Perlmutter et al., ApJ, 517, 565, 1999.
[4] J. Frieman , M. Turner and D. Huterer , ARA&A, 46, 385, 2008
[5] C. Wetterich, Nucl. Phys. B 302, 668, 1988
[6] B. Ratra and P.J.E. Peebles, Phys. Rev. D 37, 3406, 1988
[7] J.A. Frieman , C.T. Hill , A. Stebbins and I. Waga, Phys. Rev. Lett. 75, 2077, 1995
[8] M.S. Turner and M. White, Phys. Rev. D 56, R4439, 1997
[9] R.R. Caldwell , R. Dave and P.J. Steinhardt, Phys. Rev. Lett. 76, 1582, 1998
[10] P.J. Steinhardt, L. Wang , and I. Zlatev, Phys. Rev. D 59, 123504, 1999
[11] S.Tsujikawa, Lect. Notes Phys, 800, 99, 2010
[12] S. Capozziello and M. De Laurentis, Phys. Rept., 509, 167, 2011
[13] G. D. Starkman, Phil. Trans. Roy. Soc. Lond. A, 369, 5018, 2011
[14] A. Shafieloo , V. Sahni and A.A. Starobinsky, Phys. Rev. D 80, 101301, 2009
[15] M. Hicken, et al., ApJ, 700, 1097, 2009
[16] M. Chevallier and D. Polarski, Int. J. Mod. Phys. D 10, 213 , 2001
[17] E.V. Linder, Phys. Rev. Lett. 90, 091301 , 2003
[18] Z. Li , P. Wu and H. Yu, Phys. Lett. B 695, 1 , 2011
[19] R. Amanullah et al., ApJ, 716, 712, 2010
[20] V.H. Cardenas and M. Rivera, Phys. Lett. B 710, 251 , 2011
[21] V.H. Cardenas , C. Bernal and A. Bonilla, MNRAS, 433, 3534, 2013
[22] S. Sasaki , PASJ, 48, L119, 1996

[23] J. Magaña , V.H. Cardenas and V. Motta, JCAP 10, 017 , 2014
[24] I. Maor , R. Brusteinn , and P.J. Steinhardt, Phys. Rev. Lett. 86, 6 , 2001
[25] I. Maor , R. Brustein , J. McMahon , and P.J. Steinhardt, Phys. Rev. D 65, 123003 , 2002
[26] Y. Wang and P.M. Garnavich, ApJ, 552, 445 , 2001
[27] Y. Wang and G. Lovelace, ApJ, 562, L115 , 2001
[28] S.W. Allen , D.A. Rapetti , R.W. Schmidt , H. Ebeling , G. Morris and A.C. Fabian, MNRAS, 383, 879 , 2008
[29] M. Ganeshalingam, , W. Li , and A.V. Filippenko, MNRAS, 433, 2240 , 2013
[30] Planck Collaboration, P.A.R. Ade, et al., A&A 571, A22, 2014
[31] S.W. Allen , R.W. Schmidt , H. Ebeling , A.C. Fabian and L. van Speybroeck, MNRAS, 353, 457 , 2004
[32] V.R. Eke , J.F. Navarro and C.S. Frenk, ApJ 503, 569 , 1998
[33] Y. Wang , K. Freese, P. Gondolo and M. Lewis, ApJ, 594, 25 , 2003
[34] L. Perivolaropoulos, Journal of Physics Conference Series, 222, 012024 (2010).
[35] M. Ahmed, S. Dodelson, P. B. Greene and R. Sorkin, Phys. Rev. D **69**, 103523 (2004) [astro-ph/0209274].
[36] R. H. Brandenberger, hep-th/0210165.
[37] M. Quartin, M. O. Calvao, S. E. Joras, R. R. R. Reis and I. Waga, JCAP **0805**, 007 (2008) [arXiv:0802.0546 [astro-ph]].
[38] Y. Wang and K. Freese, Phys. Lett. B 632, 449 , 2006
[39] C. Blake et al., MNRAS, 418, 1707, 2011
[40] W. J. Percival et al., MNRAS, 401, 2148, 2010
[41] F. Beutler et al., MNRAS, 416, 3017, 2011
[42] Y. Wang and S. Wang, Phys. Rev. D 88, 043522 , 2013
[43] O. Lahav , S.L. Bridle , M.P. Hobson , A.N. Lasenby and L. Sodre Jr., MNRAS, 315, L45 , 2000
[44] M.P. Hobson , S.L. Bridle and O. Lahav, MNRAS, 335, 377, 2002
[45] R.A. Vanderveld , E.E. Flanagan and I. Wasserman, Phys. Rev. D 74, 023506 , 2006
[46] S. February , J. Larena , M. Smith and C. Clarkson, MNRAS, 405, 2231, 2010
[47] G.R. Bengochea and M.E. De Rossi, Phys. Lett. B 733, 258 , 2014
[48] T. Delubac *et al.* [BOSS Collaboration], A&A **574**, A59 (2015) [arXiv:1404.1801 [astro-ph.CO]].
[49] D. J. Eisenstein et al., ApJ, 633, 560, 2005
[50] D. J. Eisenstein and W. Hu, ApJ, 496, 605 , 1998
[51] W. Hu and N.Sugiyama, ApJ, 471, 542 , 1996
[52] J. R. Bond , G. Efstathiou , M. Tegmark, MNRAS 291, L33 , 1997
[53] G. Hinshaw , D. Larson , E. Komatsu , D.N. Spergel , C.L. Bennett, J. Dunkley , M.R. Nolta , and M. Halpern, et al., ApJS, 208, 19, 2012
[54] V. H. Cardenas, arXiv:1405.5116 [astro-ph.CO].
[55] V. Sahni, A. Shafieloo and A. A. Starobinsky, ApJ. **793**, no. 2, L40 (2014) [arXiv:1406.2209 [astro-ph.CO]].
[56] E. Abdalla, E. G. M. Ferreira, J. Quintin and B. Wang, arXiv:1412.2777 [astro-ph.CO].

Appendix A: Statistical Analysis

The SNIa data give the luminosity distance $d_L(z) = (1+z)r(z)$. We fit the SNIa with the cosmological model by minimizing the χ^2 value defined by

$$\chi^2_{SNIa} = \sum_{i=1}^{586} \frac{[\mu(z_i) - \mu_{obs}(z_i)]^2}{\sigma^2_{\mu i}}, \tag{A1}$$

where $\mu(z) \equiv 5\log_{10}[d_L(z)/\mathtt{Mpc}] + 25$ is the theoretical value of the distance modulus, and μ_{obs} is the corresponding observed one.

For the analysis of the gas mass fraction, following [31] using the standard priors for Ω_b, h and b mentioned in the text, the χ^2 value is

$$\chi^2_{fgas} = \sum_{i=1}^{42} \frac{(f^{\Lambda CDM}_{gas}(z_i) - f_{gas,i})^2}{\sigma^2_{fgas,i}} + \tag{A2}$$
$$+\frac{(\Omega_b h^2 - 0.02205)^2}{0.00028^2} + \frac{(h-0.72)^2}{0.08^2} + \frac{(b-0.824)^2}{0.089^2}.$$

The BAO measurements considered in our analysis are obtained from the WiggleZ experiment [39], the SDSS DR7 BAO distance measurements [40] and 6dFGS BAO data [41].

The χ^2 for the WiggleZ BAO data is given by

$$\chi^2_{WiggleZ} = (\bar{A}_{obs} - \bar{A}_{th}) C^{-1}_{WiggleZ} (\bar{A}_{obs} - \bar{A}_{th})^T, \tag{A3}$$

where the data vector is $\bar{A}_{obs} = (0.474, 0.442, 0.424)$ for the effective redshift $z = 0.44, 0.6$ and 0.73. The corresponding theoretical value $\bar{A}_{th}$ denotes the acoustic parameter $A(z)$ introduced by [49]:

$$A(z) = \frac{D_V(z)\sqrt{\Omega_m H_0^2}}{cz}, \tag{A4}$$

and the distance scale D_V is defined as

$$D_V(z) = \frac{1}{H_0}\left[(1+z)^2 D_A(z)^2 \frac{cz}{E(z)}\right]^{1/3}, \tag{A5}$$

where $D_A(z)$ is the Hubble-free angular diameter distance which relates to the Hubble-free luminosity distance through $D_A(z) = D_L(z)/(1+z)^2$. The inverse covariance $C^{-1}_{WiggleZ}$ is given by

$$C^{-1}_{WiggleZ} = \begin{pmatrix} 1040.3 & -807.5 & 336.8 \\ -807.5 & 3720.3 & -1551.9 \\ 336.8 & -1551.9 & 2914.9 \end{pmatrix}. \tag{A6}$$

Similarly, for the SDSS DR7 BAO distance measurements, the χ^2 can be expressed as [40]

$$\chi^2_{SDSS} = (\bar{d}_{obs} - \bar{d}_{th}) C^{-1}_{SDSS} (\bar{d}_{obs} - \bar{d}_{th})^T, \tag{A7}$$

where $\bar{d}_{obs} = (0.1905, 0.1097)$ are the data points at $z = 0.2$ and 0.35. $\bar{d}_{th}$ denotes the distance ratio

$$d_z = \frac{r_s(z_d)}{D_V(z)}. \tag{A8}$$

Here, $r_s(z)$ is the comoving sound horizon,

$$r_s(z) = c\int_z^\infty \frac{c_s(z')}{H(z')}dz', \tag{A9}$$

where the sound speed $c_s(z) = 1/\sqrt{3(1+\bar{R}_b/(1+z)}$, with $\bar{R}_b = 31500\Omega_b h^2(T_{CMB}/2.7\text{K})^{-4}$ and $T_{CMB} = 2.726$K.

The redshift z_d at the baryon drag epoch is fitted with the formula proposed by [50],

$$z_d = \frac{1291(\Omega_m h^2)^{0.251}}{1+0.659(\Omega_m h^2)^{0.828}}[1+b_1(\Omega_b h^2)^{b_2}], \tag{A10}$$

where

$$b_1 = 0.313(\Omega_m h^2)^{-0.419}[1+0.607(\Omega_m h^2)^{0.674}] \tag{A11}$$

$$b_2 = 0.238(\Omega_m h^2)^{0.223}. \tag{A12}$$

C^{-1}_{SDSS} in Eq. (12) is the inverse covariance matrix for the SDSS data set given by

$$C^{-1}_{SDSS} = \begin{pmatrix} 30124 & -17227 \\ -17227 & 86977 \end{pmatrix}. \tag{A13}$$

For the 6dFGS BAO data [41], there is only one data point at $z = 0.106$, the χ^2 is easy to compute:

$$\chi^2_{6dFGS} = \left(\frac{d_z - 0.336}{0.015}\right)^2. \tag{A14}$$

The total χ^2 for all the BAO data sets thus can be written as

$$\chi^2_{BAO} = \chi^2_{WiggleZ} + \chi^2_{SDSS} + \chi^2_{6dFGS}. \tag{A15}$$

We also include background CMB information by using the Planck data [30] extracted from the analysis performed by [42] to probe expansion history up to the last scattering surface. The χ^2 for the CMB data is constructed as

$$\chi^2_{CMB} = X^T C^{-1}_{CMB} X, \tag{A16}$$

where

$$X = \begin{pmatrix} l_A - 301.65 \\ R - 1.7499 \\ z_* - 1090.41 \end{pmatrix}. \tag{A17}$$

Here l_A is the "acoustic scale" defined as

$$l_A = \frac{\pi d_L(z_*)}{(1+z)r_s(z_*)}, \tag{A18}$$

where $d_L(z) = D_L(z)/H_0$ and the redshift of decoupling z_* is given by [51],

$$z_* = 1048[1+0.00124(\Omega_b h^2)^{-0.738}][1+g_1(\Omega_m h^2)^{g_2}], \tag{A19}$$

$$g_1 = \frac{0.0783(\Omega_b h^2)^{-0.238}}{1+39.5(\Omega_b h^2)^{0.763}}, g_2 = \frac{0.560}{1+21.1(\Omega_b h^2)^{1.81}}, \tag{A20}$$

The "shift parameter" R defined as [52]

$$R = \frac{\sqrt{\Omega_m}}{c(1+z_*)}D_L(z). \tag{A21}$$

C^{-1}_{CMB} in Eq. (A16) is the inverse covariance matrix,

$$C^{-1}_{CMB} = \begin{pmatrix} 42.722 & -419.68 & -0.7659 \\ -419.68 & 57394.2 & -193.808 \\ -0.7659 & -193.808 & 14.700 \end{pmatrix}. \tag{A22}$$

We have also tried the WMAP 9-yr data [53] finding no significant variation in the qualitative behavior.

For all the combinations of data mentioned in the paper, we have used the conventional joint χ^2 analysis. In this case we minimize

$$\chi^2_{total} = \sum_j \chi^2_j, \tag{A23}$$

where each χ^2_j follows the chi-square distribution. This procedure assumes that we trust the observational errors. When we combine different data sets, there is the concern about the extent to which two independent data sets are consistent with one another, with the worst scenario being when they are completely inconsistent. In such a case, one may wish to allow freedom in the relative weights. The hyper-parameter approach [43, 44] is a method that implements these ideas. Essentially the method generalizes (A23) to

$$\chi^2_{total} = \sum_j \alpha_j \chi^2_j, \tag{A24}$$

where the α_j are the weight parameter for each data set. Assuming the prior probabilities of $\log(\alpha_j)$ are uniform, and after marginalizing over these parameters, the posterior probability (in its gaussian form) can be written in terms of the original χ^2_j in such a way that one should consider minimizing

$$\chi^2_{hyper} = \sum_j N_j \ln \chi^2_j, \tag{A25}$$

instead of (A23). Here N_j is the number of data points of the corresponding data set.